

Crystallization of the metallic glass $\text{Fe}_{78}\text{B}_{13}\text{Si}_9$

J. Y. BANG, R. Y. LEE

Department of Materials Science and Engineering, Dankook University, Cheonahn 330-714, Korea

The microstructures and kinetics with heating for an amorphous $\text{Fe}_{78}\text{B}_{13}\text{Si}_9$ alloy were studied by X-ray diffraction, transmission electron microscopy, differential thermal analysis and differential scanning calorimetry. The first crystallization takes place by the simultaneous formation of α -(Fe,Si) and Fe_3B having the shapes of dendrite and spherulite, respectively. Metastable Fe_3B then transformed into a stable phase of Fe_2B at a higher temperature. The activation energy for crystallization and the Avrami exponent were determined. It was found that crystallization behaviour in $\text{Fe}_{78}\text{B}_{13}\text{Si}_9$ is controlled by nucleation rather than growth.

1. Introduction

Metallic glasses have attracted considerable attention from materials and scientific communities, because of their technologically interesting properties. For application of these materials, a detailed knowledge of the crystallization and kinetic behaviours is thus very important. The most intensively studied glasses are the binary ones, especially $\text{Fe}_{1-x}\text{B}_x$ [1]. Two types of crystallization process have been observed for these simple binary alloys.

Recently, it has been found [2] that the addition of Si into the Fe–B system enhances the thermal stability in metallic glass. As far as thermal stability is concerned, the most favourable Fe–B–Si glasses have 5 to 10 at % Si and 75 to 78 at % Fe, and indeed, glasses with the greatest technological significance fall in this region. For Fe–B–Si amorphous alloys, the phases initially formed were dependent upon alloy composition and, in addition, great differences in crystallization morphology were found [3]. Contradictory results in the crystallization sequences for the same composition have also been reported in the literature [4, 5]. Nevertheless comprehensive studies both on the microstructures and kinetics of $\text{Fe}_{78}\text{B}_{13}\text{Si}_9$ metallic glasses have not been undertaken. A detailed study of the crystallization behaviour of $\text{Fe}_{78}\text{B}_{13}\text{Si}_9$ is thus greatly needed for better understanding and application of this material.

In the present experiment the transformation from the amorphous to the crystalline state with heating for $\text{Fe}_{78}\text{B}_{13}\text{Si}_9$ is thoroughly investigated with X-ray diffraction (XRD), transmission electron microscope (TEM), differential thermal analysis (DTA), and differential scanning calorimeter (DSC), to elucidate the crystallization and kinetic behaviour of this metallic glass.

2. Experimental procedure

The $\text{Fe}_{78}\text{B}_{13}\text{Si}_9$ amorphous alloy (Metglass 2605-S2) studied was kindly supplied, in ribbon form 10 mm wide and 25 μm thick, by Osaka University. The

initial amorphous state of the sample used in this experiment was confirmed by XRD and TEM. Heat treatments were conducted in a vacuum furnace at temperatures between 400 and 600 °C for 30 to 120 min. No oxidation was observed after thermal heating. The crystalline phases were identified using both XRD with CrK_α radiation and selected area diffraction (SAD) in TEM (Jeol 100CX). The specimens for TEM were prepared using the modified Ballman-window technique. The samples for TEM were thinned by electropolishing in an electrolyte consisting of 20% perchloric acid in ethylalcohol while maintaining a temperature of less than 233 K by using an immersion cooler (Flexi-Cool). The kinetic behaviour of $\text{Fe}_{78}\text{B}_{13}\text{Si}_9$ was studied using Rigaku DTA (PTC-10A) and Perkin-Elmer DSC-7 under an inert atmosphere of N_2 gas.

3. Results and discussion

3.1. Structure analysis

The $\text{Fe}_{78}\text{B}_{13}\text{Si}_9$ alloy remained amorphous with heating up to 673 K. Fig. 1a shows XRD trace for the sample heated at 723 K for 30 minutes. As can be seen the very small peaks corresponding to the crystalline phases of α -(Fe,Si) and Fe_3B appeared at this temperature. After 120 minutes at the same temperature, the well established Bragg's peaks of these crystalline phases with no traces of Fe_2B are observed (Fig. 1b) as expected. Diffractometric phase analysis showed that the crystallization stage was characterized by the simultaneous formation of α -(Fe, Si) and Fe_3B . This observation is consistent with those of Quivy *et al.* [3] and Ramanan and Fish [2]. These results, however, differ from those of Zaluska *et al.* [5] and Surinach *et al.* [4]. The later investigators reported that the crystallization stage was characterized by the primary crystallization of α -(Fe,Si) and followed by eutectic crystallization. On the other hand, according to Zaluska's diagram, which is not always correct [6] for anticipating the crystalline sequence in the ternary Fe–B–Si systems, the alloy $\text{Fe}_{78}\text{B}_{13}\text{Si}_9$ should be

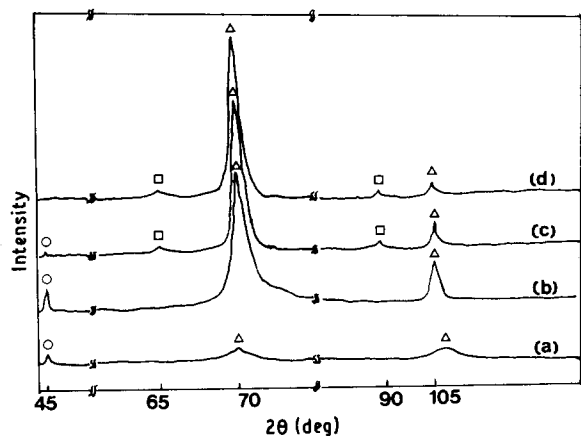


Figure 1 X-ray diffraction patterns of $\text{Fe}_{78}\text{B}_{13}\text{Si}_9$ with heat treatment at (a) 723 K for 30 min, (b) 723 K for 2 h, (c) 773 K for 2 h, and (d) at a higher temperature of 823 K for 1 h. (Δ α -(Fe,Si), \square Fe_2B , \circ Fe_3B).

characterized by crystallization of α -(Fe, Si) and Fe_2B . The reason for this slightly different crystallization sequence found for the same $\text{Fe}_{78}\text{B}_{13}\text{Si}_9$ alloy is not clear but it might be associated with the different manufacturing methods which have different quenched nuclei in the amorphous.

Fig. 1c is the XRD pattern for the specimen annealed at 773 K for 120 minutes. Compared with Fig. 1b, the diffraction peak height to the metastable phase of Fe_3B at $2\theta = 46.2^\circ$ decreased, while very

small peaks corresponding to the stable Fe_2B phase appeared at $2\theta = 65.4^\circ$ and 89.3° . After annealing at the higher temperature of 823 K for 60 min, (Fig. 1d) the metastable Fe_3B phase had totally disappeared because of the transition into a more stable phase of Fe_2B . XRD analysis at this temperature showed that the crystallization products of amorphous $\text{Fe}_{78}\text{B}_{13}\text{Si}_9$ alloy were two-phase mixtures of α -(Fe,Si) and Fe_2B .

3.2. Microstructure of crystalline phase

In spite of great interest in the crystallization of Fe-B-Si glass, only a few micrographs presenting this process have so far been published [7, 8]. In order to clarify in more detail the transformation from the amorphous to crystalline phases, TEM observations of microstructural changes during heat treatment were carried out. Fig. 2a and b show the TEM images after heat treatment at 723 K. Two kinds of crystal with different shapes are simultaneously shown in these figures. The selected area diffraction (SAD) analysis on these crystals shows that two crystal forms of solid solution α -(Fe,Si) and metastable Fe_3B exist which is consistent with XRD results. Fig. 2c is the SAD pattern for star-like or dendrite identified as α -(Fe,Si). This kind of morphology is similar to that reported by Chang *et al.* [9] and Swartz *et al.* [10]. The SAD pattern on the other cuboidal shape is shown in Fig. 2d. It is determined to be Fe_3B . This shape is also

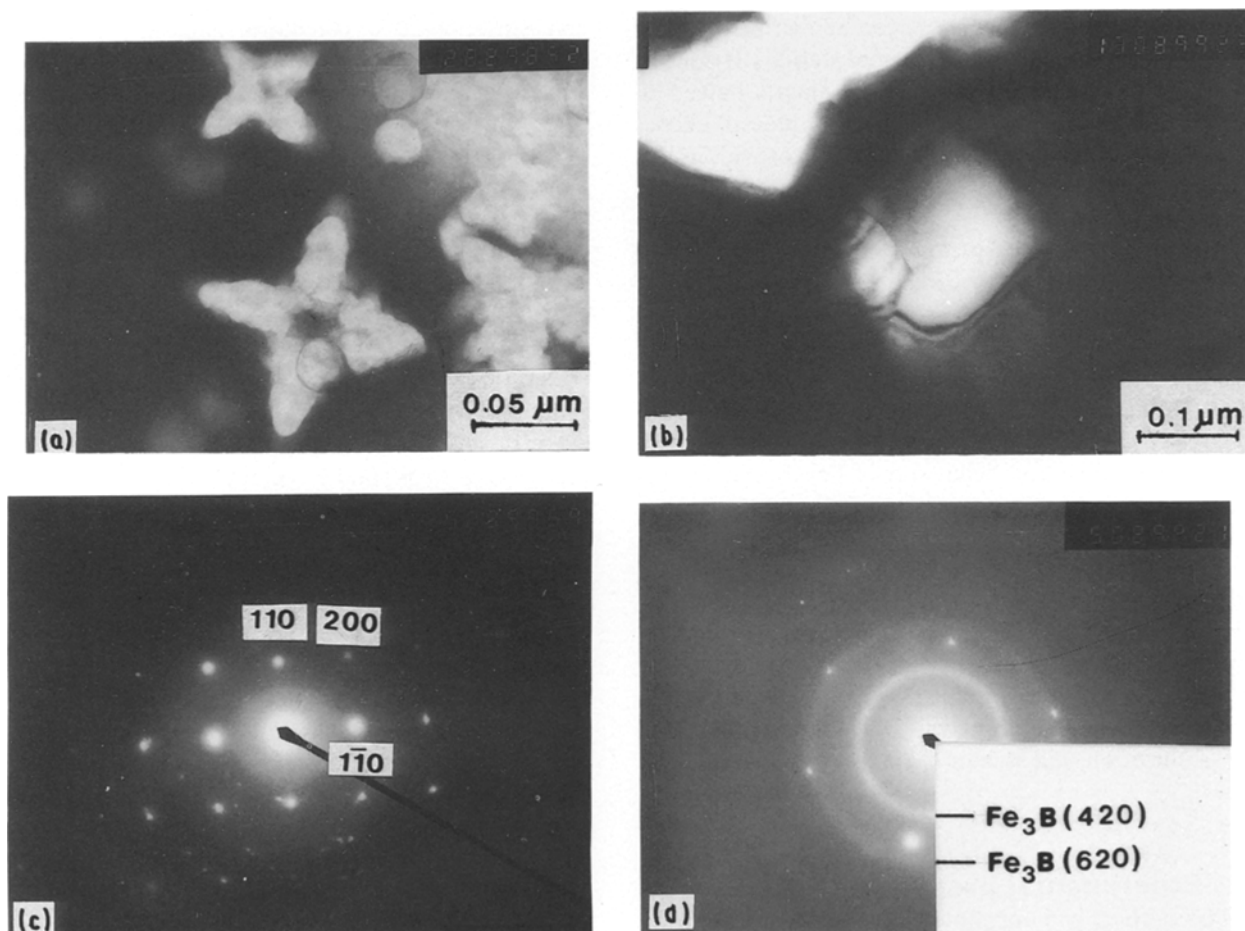


Figure 2 (a) (c) Transmission electron micrographs and their (b) (d) diffraction patterns for α -(Fe,Si) and Fe_3B phases formed after annealing at 723 K for 60 min in $\text{Fe}_{78}\text{B}_{13}\text{Si}_9$ alloy.

very similar to the Fe_3B crystals formed during crystallization of binary Fe-B amorphous alloy [11].

Fig. 3 is the micrograph for spherulite which formed at a higher annealing temperature of 773 K for 60 min. Compared with the cuboidal shape with no detectable microstructure in Fig. 2b, the microcolumns have evidently developed within the spherulite formed at the higher temperature of 773 K. Fe_3B is itself metastable and decomposes into $\alpha\text{-(Fe,Si)}$ and Fe_2B on further heating. The microstructure is shown after annealing at 823 K for 60 min in Fig. 4a. The SAD pattern shown in Fig. 4b is identified as a stable Fe_2B which is coincided with the results of XRD.

3.3. Microhardness

Microhardness measurements were made with heating to study the effect of crystallization on the mechanical property. Ten measurements were made at room temperature on each specimen and then mean values were taken to report the result. The Knoop hardness values were plotted as a function of annealing temperature as shown in Fig. 5. The hardness increases with heating up to 823 K and then it decreases. Microstructure observations by TEM and XRD showed that crystalline products were formed in the temperature range between 673 and 773 K. The increased microhardness is thus thought to have arisen from the precipitation hardening of crystalline phases in the amorphous matrix. At temperatures greater than 823 K the microstructure is composed of stable crystalline phases of $\alpha\text{-(Fe,Si)}$ and Fe_2B . The coarsening of these phases at a higher annealing temperature also leads to a decrease in hardness.

3.4. Kinetics for crystallization

Fig. 6 shows the DTA recordings obtained for $\text{Fe}_{78}\text{B}_{13}\text{Si}_9$ metallic alloy with various heating rates. The thermograms exhibit two distinct peaks of crystallization. Two peak temperatures (T_p) shift their positions with heating rate. The apparent activation energies (E_a) for crystallization were determined by Augis-Bennet [12] plots of $\ln[(T_p - 298)/\phi]$ against

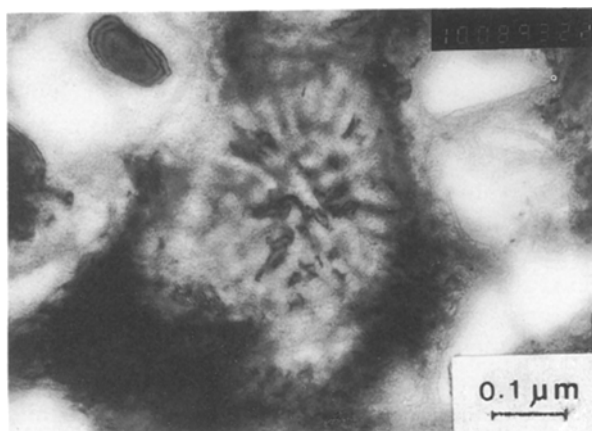


Figure 3 Transmission electron micrograph shows that the microcolumns are developed within the Fe_3B spherulite after heating at 773 K for 1 h.

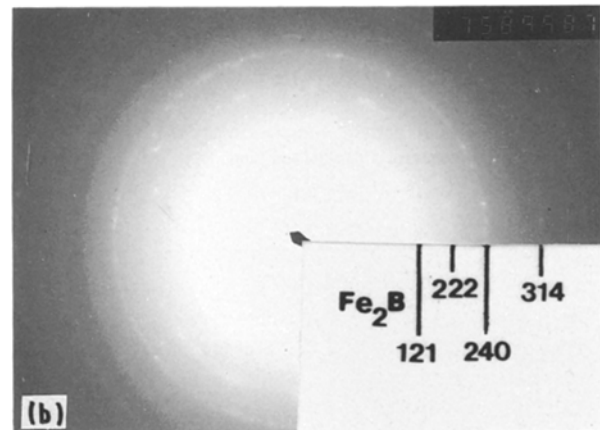
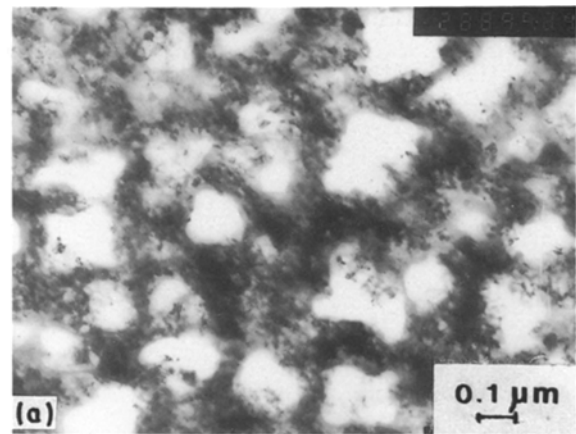


Figure 4 (a) Transmission electron micrograph and (b) its diffraction pattern for Fe_2B after annealing at 823 K for 60 min.

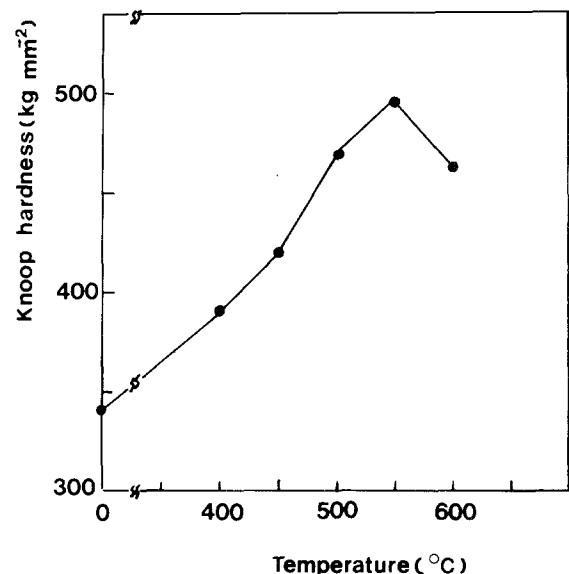


Figure 5 The change in Knoop microhardness with annealing temperature for amorphous $\text{Fe}_{78}\text{B}_{13}\text{Si}_9$ (load 10 g).

$1/T_p$ where ϕ is the heating rate. The apparent activation energies determined from Fig. 7 using the least square method are 106 and 77 kcal mol⁻¹ for the first and second peak, respectively. The first activation energy of 106 kcal mol⁻¹ is in good agreement with Surinach *et al.* [4] and the extracted value from contours of constant activation energy displayed by Ramanan and Fish [2] in Fe-B-Si system, while the

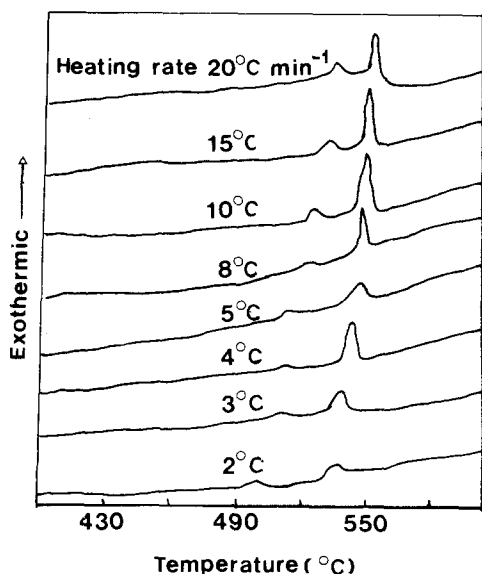


Figure 6 Differential thermal analysis recordings of the metallic glass $\text{Fe}_{78}\text{B}_{13}\text{Si}_9$ obtained at various heating rates.

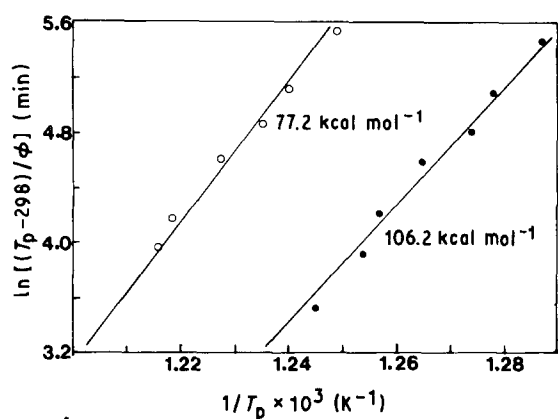


Figure 7 Augis-Bennet plots of exothermic peak temperature for determining the activation energies of crystallization for $\text{Fe}_{78}\text{B}_{13}\text{Si}_9$ alloy. (● First peak, ○ second peak).

second activation energy determined in the present experiment differs with them. The Avrami [13] exponent n was obtained by Ozawa [14] plots of $\ln[-\ln(1-X)]$ against $\ln t$ where X is the crystalline fraction at time t , by assuming that the total heat evolved is proportional to X during the course of an isothermal annealing at 773 K. The exponent n is determined to be 2.1 and 2.3 for the first and the second crystallizations, respectively.

The activation energy for the eutectic crystallization in Fe-B glass has been found to be about 50 kcal mol^{-1} [15, 16]. Compared to this, the determined activation energy for the eutectic crystallization in $\text{Fe}_{78}\text{B}_{13}\text{Si}_9$ glass has a higher value of $106 \text{ kcal mol}^{-1}$, which indicated that the addition of metalloid Si atoms into Fe-B system enhances the thermal stability in Fe-B-Si glass and is in agreement with Ramanan and Fish [2]. It has been reported that the solubility of B and Si in α -iron at 723 K is below 0.01 and 10 at %, respectively [17]. The nucleation and growth of α -(Fe,Si) and Fe_3B in amorphous $\text{Fe}_{78}\text{B}_{13}\text{Si}_9$ thus involve local arrangement of Fe and Si and long diffusion of B. The higher activation energy for crystallization in ternary $\text{Fe}_{78}\text{B}_{13}\text{Si}_9$ glass than that of

binary Fe-B glass is associated with the higher energy barrier for B diffusion with the presence of a substitutional Si atom in an Fe site.

The crystallization of metallic glass is a nucleation and growth process. Since the growth processes in Fe-B and Fe-B-Si glass systems are known to be diffusion controlled [9, 16], we infer that such is also the case for $\text{Fe}_{78}\text{B}_{13}\text{Si}_9$ glass. It has been shown [2] that for various nucleation and growth mechanisms, a useful picture of the diffusion controlled crystallization process emerges if n is partitioned as $n = a + b/2$, where a refers to the nucleation rate and varies from 0 to 1, and b represents the dimensionality of the crystal growth. Here b is assigned the value 3 because of the three dimensionality of crystalline products of α -(Fe,Si), Fe_3B and Fe_2B . The traditional interpretation for the Avrami exponent of 2.1 and 2.3 is, therefore, that crystallization is governed by the diffusion controlled growth with a decreasing nucleation rate ($a = 0.6$).

Furthermore the apparent activation energy (E_a) was formulated [18] as follows for diffusion controlled three-dimensional growth: $E_a = aE_n + 1.5E_d$, where E_n and E_d are the activation energies for nucleation and diffusion, respectively. By substitution the determined values of $E_a = 106 \text{ kcal mol}^{-1}$ and $a = 0.6$ for the first crystallization and the reported value [9] of $E_d = 37 \text{ kcal mol}^{-1}$ for boron into this equation, the activation energy for nucleation is found to be about 84 kcal mol^{-1} . Although this calculation, without any detailed kinetic study with TEM, is not sufficient to say anything about the crystallization kinetics, one can easily conclude that the first crystallization process in $\text{Fe}_{78}\text{B}_{13}\text{Si}_9$ metallic alloy is controlled by nucleation rather than growth.

4. Conclusion

The crystallization behaviour of the metallic glass $\text{Fe}_{78}\text{B}_{13}\text{Si}_9$ studied using XRD, TEM, DTA and DSC showed that the first crystallization occurred at 723 K and was always characterized by the simultaneous formation of solid solution α -(Fe,Si) and metastable Fe_3B having the morphology of star-like and cuboidal shapes, respectively. The microcolumn of Fe_3B developed within the spherulite formed at a higher temperature of 773 K. At a higher temperature of 823 K the metastable Fe_3B transformed into the stable phase of Fe_2B . The precipitation hardening of crystalline phases in an amorphous matrix results in an increase in hardness with heating and then it decreases at a higher temperature due to the coarsening of these phases and the formation of a stable crystalline phase. The activation energies were determined to be 106 and 77 kcal mol^{-1} for the first and second crystallizations, respectively. The Avrami exponents were also found to be 2.1 and 2.3 for each stage of crystallization. The first eutectic crystallization in $\text{Fe}_{78}\text{B}_{13}\text{Si}_9$ metallic glass was found to be controlled by nucleation rather than growth, thus the higher thermal stability in $\text{Fe}_{78}\text{B}_{13}\text{Si}_9$ than that of Fe-B binary system was associated with the suppression of nucleation with the addition of silicon.

References

1. T. NAKAJIMA, I. NAGAMI and H. INO, *J. Mater. Sci. Lett.* **5** (1986) 60.
2. V. R. V. RAMANAN and G. E. FISH, *J. Appl. Phys.* **53** (1982) 2273.
3. A. QUIVY, J. RZEPSKI, J. CHEVALIER and Y. CALVAYRAC, in *Proceeding of the 5th International Conference on Rapidly Quenched Metals*, Amsterdam (1985), edited by S. Steeb and H. Warlimont, p. 15.
4. S. SURINACH, M. D. BARO and N. CLAVAGUERA, *ibid.* p. 323.
5. A. ZALUSKA and H. MATAJA, *J. Mater. Sci.* **18** (1983) 2163.
6. K. HOSELITZ, *Phys. Status Solidi a* **53** (1979) K23.
7. A. INOUE, T. MASUMOTO, M. KIKUCHI and T. MINE-MURA, *J. Jpn Inst. Met.* **42** (1978) 294.
8. A. DATTA, N. J. de CRISTOFARO and L. A. DAVIS, in *Proceeding of the 4th International Conference on Rapidly Quenched Metals*, Japan (1981) edited by J. Masumoto and X. Suzuki, p. 1007.
9. C. F. CHANG and J. MARTI, *J. Mater. Sci.* **18** (1983) 2297.
10. C. F. SWARTZ, R. KOSSOWSKY, J. J. HAUGH and R. F. KRAUSE, *J. Appl. Phys.* **52** (1981) 3324.
11. J. L. WALTER, S. F. BARTRAM and R. R. RUSSEL, *Met. Trans.* **9A** (1978) 803.
12. J. A. AUGIS and J. E. BENNET, *J. Thermal Anal.* **13** (1978) 283.
13. M. AVRAMI, *J. Chem. Phys.* **7** (1939) 1103.
14. T. OZAWA, *Polymer* **11** (1970) 150.
15. U. HEROLD and U. KOSTER, in "Rapidly Quenched Metals" Vol. 1, edited by B. Cantor (Metals Society, London, 1979) p. 281.
16. U. KOSTER, U. HEROLD, H. G. HILLENBRAND and J. DENIS, *J. Mater. Sci. Lett.* **15** (1980) 2125.
17. M. HANSEN, "Constitution of Binary Alloys" (McGraw-Hill, New York, 1958).
18. S. RANGANATHAN and M. VON HEIMENDAHL, *J. Mater. Sci.* **16** (1981) 2401.

*Received 11 June 1990
and accepted 31 January 1991*